Biochimica et Biophysica Acta 1818 (2012) 1211–1217

Contents lists available at SciVerse ScienceDirect

Biochimica et Biophysica Acta

journal homepage: www.elsevier.com/locate/bbamem

Probing the interaction between heparan sulfate proteoglycan with biologically relevant molecules in mimetic models for cell membranes: A Langmuir film study

Luciano Caseli [a,*], Renan Pelluzzi Cavalheiro [b], Helena B. Nader [b], Carla Cristina Lopes [a,b]

[a] Instituto de Ciências Ambientais, Químicas e Farmacêuticas, Universidade Federal de São Paulo, Diadema, SP, Brazil
[b] Escola Paulista de Medicina, Universidade Federal de São Paulo, São Paulo, SP, Brazil

ARTICLE INFO

Article history:
Received 14 October 2011
Received in revised form 2 January 2012
Accepted 13 January 2012
Available online 21 January 2012

Keywords:
Heparan sulfate proteoglycan
Syndecan-4
Molecular recognizing
Langmuir monolayer

ABSTRACT

Investigating the role of proteoglycans associated to cell membranes is fundamental to comprehend biochemical process that occurs at the level of membrane surfaces. In this paper, we exploit syndecan-4, a heparan sulfate proteoglycan obtained from cell cultures, in lipid Langmuir monolayers at the air–water interface. The monolayer served as a model for half a membrane, and the molecular interactions involved could be evaluated with tensiometry and vibrational spectroscopy techniques. Polarization–modulation infrared reflection–absorption spectroscopy (PM-IRRAS) employed in a constant surface pressure regime showed that the main chemical groups for syndecan-4 were present at the air–water interface. Subsequent monolayer decompression and compression showed surface pressure-area isotherms with a large expansion for the lipid monolayers interacting with the cell culture reported to over-express syndecan-4, which was also an indication that the proteoglycan was inserted in the lipid monolayer. The introduction of biological molecules with affinity for syndecam-4, such as growth factors, which present a key role in biochemical process of cell signaling, changed the surface properties of the hybrid film, leading to a model, by which the growth factor binds to the sulfate groups present in the heparan sulfate chains. The polypeptide moiety of syndecan-4 responds to this interaction changing its conformation, which leads to lipid film relaxation and further monolayer condensation.

1. Introduction

Syndecans, heparan sulfate proteoglycans (HSPGs), are abundant molecules associated with the cell surface and extracellular matrix and consist of a protein core to which heparan sulfate chains are covalently attached. Invertebrates and primitive chordates possess a single syndecan gene while mammals have four syndecan genes that are divided into two subfamilies consisting of syndecan-1 and -3, and -2 and -4, respectively [1–4]. Syndecans are type I membrane glycoproteins, having three major domains, named ectodomain, transmembrane and cytoplasmic. The amino-terminal sequence of the core protein is followed by an ectodomain containing Ser–Gly consensus sequences for the glycosaminoglycan attachment, a single highly conserved transmembrane domain, and a short highly conserved cytoplasmic domain. All syndecan proteins carry heparan sulfate chains, and some core proteins can be additionally substituted with chondroitin sulfate chains [5–9].

Syndecan core proteins range in size from 20 to 45 kDa and form stable dimers as a result of interactions within their transmembrane domains. Central to this is a highly conserved GXXXG motif, which is common to syndecan transmembrane domains from all species [10–12]. The transmembrane domains are relatively stable evolutionarily, since only a few amino acids differ among the vertebrate sequences. These domains contain regions for interactions with other membrane proteins and for localization to distinct membrane compartments [8].

The cytoplasmic domains contain two invariant regions, a membrane proximal common region (C1) containing a serine and a tyrosine and a C-terminal common region (C2), separated by a region (V) of variable length and composition. The C2 region shows an EFYA sequence at the C-terminus that can bind to the PDZ domain present in specific proteins. PDZ domains, named for PSD-95, Discs-large, and Zonula occludens-1 proteins, bind specific C-terminal sequences and organize and assemble protein complexes on the inner surface of the plasma membrane and are thought to link membrane components to the underlying actin-containing cytoskeleton. The variable (V) region is distinct for each of the 4 family members, but its syndecan specific identity is conserved across species [3]. The function of this domain is largely unknown except for syndecan-4, where it is responsible for the assembly of syndecan-4 tetramers

Abbreviations: PM-IRRAS, polarization–modulation infrared reflection–absorption spectroscopy; HSPGs, heparan sulfate proteoglycans; EGF, epidermal growth factor; EC, endothelial cell; EJ-*ras* EC, Endothelial cell transfected with EJ-ras oncogene; shRNA-Syn4-EC, EC transfected with plasmid vector for the expression of RNA interference to syndecan-4; DPPC, dipalmitoylphosphatidylcholine

* Corresponding author. Tel.: +5511 3319 3300; fax: +5511 4043 6428.
E-mail address: lcaseli@unifesp.br (L. Caseli).

0005-2736 © 2012 Elsevier B.V. Open access under the Elsevier OA license.
doi:10.1016/j.bbamem.2012.01.012

with phosphatidylinositol 4,5-bisphosphate (PIP2) and activated protein kinase C-α (PKC-α) in focal adhesions [8,13,14]. Syndecan-4 cytoplasmic domain is amenable to NMR spectroscopy, and forms a stable dimer of unusual characteristics. It forms a twisted clamp, and some of the key residues that stabilize the structure are at either end of the V region [9,15].

In this sense, it is interesting to investigate the role of syndecan-4 in simplified models of cell membranes in order to access molecular interactions. An interesting approach to artificially construct cell membrane surfaces is employing the Langmuir technique, which consists of spreading insoluble amphiphiles on the air–water interface allowing for the formation of a monomolecular film named Langmuir monolayer [16]. This film can contain its composition and also its surface density experimentally controlled. Once formed, techniques involving surface chemistry, such as surface tensiometry, surface potential, microscopy and light absorption spectroscopy, may be employed to investigate the physical chemical parameters involved. Also, hybrid monolayers can be constructed either by spreading mixed insoluble amphiphiles or by injecting soluble materials into the aqueous subphase, and allowing for the adsorption of these materials (such as proteins, drugs, and nucleic acids) from solution to the previously formed monolayer.

Hence hybrid protein–lipid monolayers are useful to mimic half a membrane as defended in the 1990s [17], this technique has been also used to investigate interactions involved in molecular recognizing events [18–21], to construct hybrid films of enzymes for biosensing [22–24], and to investigate natural polysaccharide fibers [25]. Also has this technique been shown as a potent tool for studying the interfacial properties of antimicrobial and membrane-lytic peptides and their interactions with lipid membranes [26–28]. Despite being able to mimic half a membrane, and being therefore particularly useful to investigate interactions with peripheral proteins, also monolayers at the air–water interface have been employed to study interactions of transmembrane proteins with cells [29].

Thus Langmuir monolayers are particularly adequate to investigate interactions of syndecan-4 with lipids at biointerfaces, since we are leading with a class of molecules associated with cell surfaces and extracellular matrices. To the best of our knowledge, syndecan-4 has never been investigated in Langmuir monolayers, although some studies have reported the interaction of syndecans in other cell models, such as liposomes [30,31]. Also, other proteoglycans interacting with lipid Langmuir monolayers have been investigated, such as arabinogalactan [32], sulfated saccharides interacting with cardiotoxins [33] or lipids [34], and sugar-binding proteins, such as lectins [35].

This present work aims to investigate the incorporation of syndecan-4 in lipid monolayer acting as a cell membrane model. As we have employed lipid monolayers, which are systems that mimic half a membrane [17], we intended to focus our study on the ectodomain of the protein. Three samples of cell extracts containing different amounts of syndecan-4, one of which is tumorigenic cell lines, were used. Also we investigated processes of molecular recognizing in which it is believed syndecan-4 to be involved. For that, we have employed biological molecules for which interactions with syndecan-4 are reported, such as, heparin, and epidermal growth factor (EGF). Specific regions of biomolecule's interaction on syndecan-4 moieties were inferred from data obtained from surface chemistry (tensiometry and polarization modulation infrared reflection–absorption spectroscopy: PM-IRRAS).

2. Materials and methods

2.1. Heparan sulfate and growth factor

Heparan sulfate from bovine pancreas was a gift from the late Dr. P Bianchini (Opocrin Research Laboratories, Modena, Italy). Epidermal growth factor (EGF) was acquired from Sigma-Aldrich.

2.2. Cell culture

Endothelial cell line derived from rabbit aorta (EC) [36], EC transfected with EJ-*ras* oncogene (EJ-*ras* EC) [37] and EC transfected with plasmid vector for the expression of RNA interference to syndecan-4 (shRNA-Syn4-EC) (unpublished data) were grown in F-12 medium (Gibco BRL, Grand Island, USA) supplemented with 10% fetal calf serum (FCS) (Cultilab, Campinas, SP, Brazil) in the presence of penicillin (100 U/mL) and streptomycin (100 μg/mL). They were grown at 37 °C in a humidified, 2.5% CO_2 atmosphere and sub-cultured every week with Pancreatin (Sigma-Aldrich, St. Louis, MO, USA).

2.3. Extraction of syndecan-4

Proteoglycans synthesized by the cells were metabolically labeled with [^{35}S]-sulfate (150 μCi/mL) in F-12 medium for 18 h at 37 °C in 2.5% CO_2 atmosphere. Afterward, the culture medium was removed and the cells washed twice with F-12 medium and scrapped from the dish with 3.5 M urea in 25 mM Tris–HCl pH 7.8. Syndecan-4 was identified and quantified by agarose gel electrophoresis, as previously described in [37,38]. Syndecan-4 was located by exposure of the gels (after fixation, drying and staining) to Kodak X-ray film (SB-5) for 3–15 days. The samples of lipids and commercial proteins used in this work had purity above 99%. Extract of syndecans was not further purified in order to not interfere with the synergistic process involved in their interaction with membranes. Also, we intend to avoid relevant alterations to the secondary and tertiary structures of the protein owing to the further process of purification.

2.4. Langmuir monolayers

Langmuir monolayers were obtained spreading a chloroform (Sigma) solution of dipalmitoylphosphatidylcholine (DPPC), purchased from Sigma-Aldrich, on the surface of a buffer aqueous solution (Tris 25 mmol/L, urea 3.5 M; pH correct to 7.8 with diluted HCl; all from Sigma-Aldrich). The lipid concentration was 0.7 mmol/L, and the spread volume as 50 μL, rendering 2.1×10^{16} molecules at the surface. Water employed was previously purified by a MilliQ-Plus System (resistivity 18.2 MΩ cm, pH 5.5). Surface pressure-area (π-A) isotherms were obtained in a mini-KSV Langmuir trough, equipped with a surface pressure sensor (Wilhelmy method), with interface compression rate at 5 Å^2 molecule^{-1} min^{-1}. After 20 min. allowed for chloroform evaporation, the DPPC monolayer was compressed until the surface pressure of 30 mN/m, and then the proteins and saccharides studied in this work were injected in the aqueous subphase behind the trough barriers to avoid monolayer disturbance, and allowed for stabilization for 1 h. The stabilization has been checked with PM-IRRAS spectroscopy until no signal variation of signal is detected. Also, the surface pressure was kept constant at 30 mN/m by moving the barriers, and the stabilization of the monolayer was also checked until no movement of the barriers was more needed. Consequently, these experiments were carried out at constant surface pressure regime. PM-IRRAS measurements were taken with a KSV PMI 550 instrument (KSV Instrument Ltd, Helsinki, Finland) at a fixed incidence angle of 75°. To evaluate as syndecan shifts the monolayer to large areas and also to investigate the mixed monolayer in all 2-D states reachable by the monolayer, from expanded phases to the collapse, surface pressure-area isotherms were obtained. For that, the monolayer was then expanded to the maximum area allowed for the Langmuir trough and then compressed to collapse. All the experiments were carried out at a controlled room temperature (25 °C).

3. Results and discussion

Fig. 1 shows the infrared absorption bands for mixed DPPC-syndecan-4 monolayers obtained at 30 mN/m. To minimize the

influence of the bands for DPPC that fits in the range portrayed in these spectra, the spectrum for pure DPPC, which presents two main bands at 1730 cm^{-1} (C═O stretch in ethers) and 1240 cm^{-1} (P═O stretch in phosphate), was taken as subtracted background. With introduction of EC extract in the monolayer, the bands related to amide in polypeptides are presented. The one at 1522 cm^{-1} is related to amide II (H–N–C bends) and the ones at 1670, 1647 and 1614 cm^{-1} are related to amide I (C═O stretches), in β-turns, unordered and β-sheet structures respectively. These results therefore reflect the secondary structure of the protein inserted in the monolayer. As vibration transition for H–O–H bend for water absorbs in the range of 1650–1700 cm^{-1} [39], the group of bands for amide I turns negative because of the difference of the reflectivity between the air–water interface covered with DPPC and with DPPC-syndecan-4, reflecting therefore loss of interfacial water molecules. This is an indicative that the heparan sulfate chains attached to syndecam-4 replace some interfacial water molecules. This result is another evidence therefore that syndecan-4 was incorporated at the interface. The bands in 1245 and in 1267 cm^{-1} are related to S═O stretches in alkyl sulfate ethers and salts, groups present in the heparan sulfate chains. These bands probably overlap the ones for phosphate groups in DPPC. Hence it is reasonable to assume that these bands may be attributed to sulfate and not for DPPC because: i) spectrum for pure DPPC monolayer is subtracted in the normalized spectra; ii) the bands for phosphate that appeared for pure DPPC monolayer is about 10-fold smaller than the ones obtained with syndecan-4; and iii) it is reported in the literature that the band for asymmetric P═O stretching of PO_2 (centered at 1269 cm^{-1}) is overlapped by asymmetric stretching bands of S═O, which is centered at 1239 cm^{-1} [34].

Interestingly, the position of the amide I bands reflects the secondary structure of the proteins inserted in the monolayer. It has been reported that for syndecan-4 a typical β-sheet protein containing only minor amounts of α-helix [40], with 45% of amino acids to reside in β-sheets and less than 5% in α-helices, and the remaining amino acids being part of loops. As a strong negative band has appeared because of the water molecule replacement by syndecan-4, it is difficult to establish a relationship between the secondary structure components. However, we observe that the protein at the monolayer is structured mainly in β-structures, as reported in the literature [40].

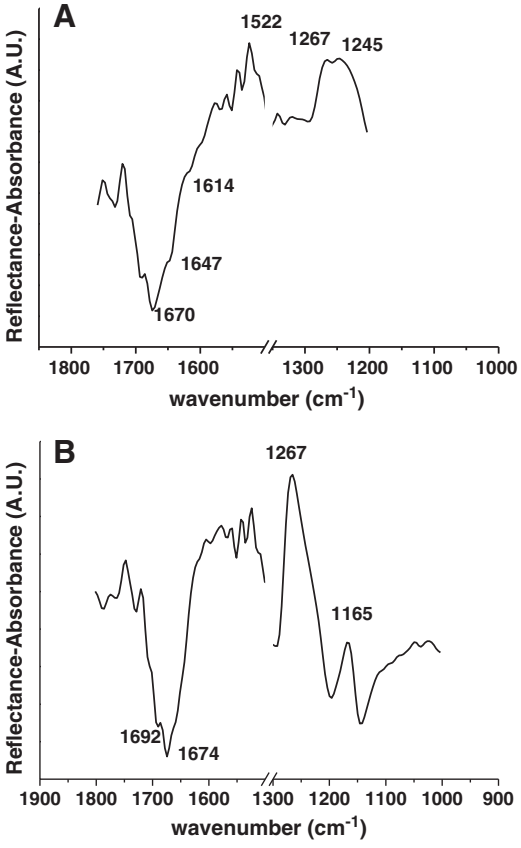

Fig. 1. PM-IRRAS spectra for DPPC monolayers at 30 mN/m with EC (A) and EJ-ras EC (B), as subphase, both at concentrations of 25 μg/L. The spectra were normalized with pure DPPC monolayer taken as background.

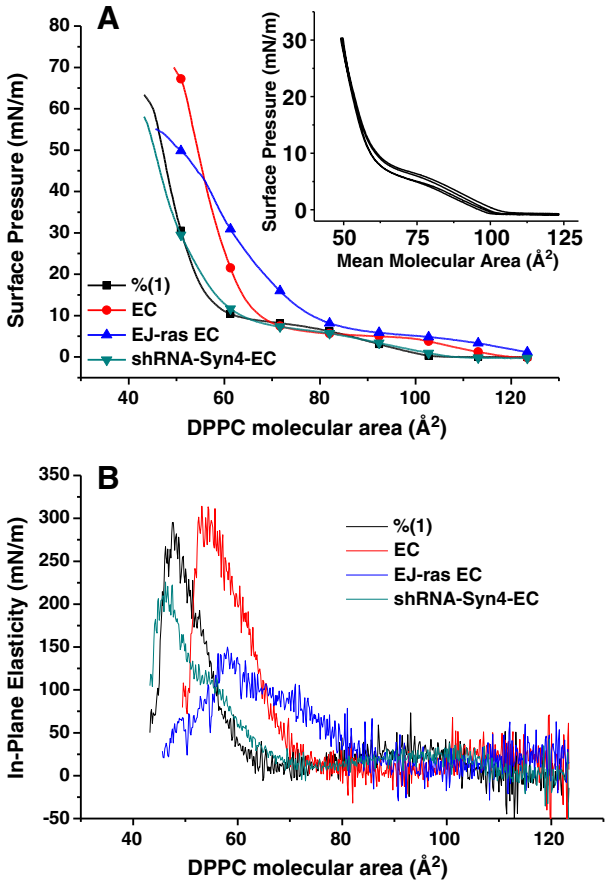

Fig. 2. Surface pressure-area isotherms (A) and In-plane elasticity-area isotherms (B) for DPPC monolayers on aqueous subphase of samples with probable expression of syndecan-4 (25 μg/L).The kind of syndecan extract is indicated in the insets. Superior inset in Panel A shows the absence of hysteresis through compression–decompression curves.

For EJ-*ras* EC, the bands shown in Fig. 2B reveal α-helix structures (shoulder at 1653 cm^{-1}), and also the presence of sulfates (strong band at 1267 cm^{-1}). The band at 1165 cm^{-1} that appeared for EJ-*ras* EC can be attributed to C–O–C in glycosyl groups. For EC, the bands were too small, being confounded with noises in the spectra. This makes therefore more evident that the substance that is being incorporated in the monolayer is a heparan sulfate proteoglycan–syndecan-4. The higher amount incorporated when 4H was used as subphase confirms the fact that this cellular line expresses higher amounts of syndecan-4.

The infrared spectrum for DPPC on a shRNA-Syn4-EC subphase is practically coincident with the fingerprint for pure DPPC. No significant bands for amide, glycosyl or sulfate groups are present, revealing neglecting adsorption of glycoproteins at the DPPC monolayer. With the normalization employed, we have obtained a straight line spectrum, and for the sake of clarity, it is not shown.

As the extract contained other biological molecules that are important to maintain the structure and function of syndecan, we inserted a growth factor and heparin in the lipid monolayers to identity whether, in fact, the effects observed in the surface pressure-area

isotherms, which will be shown below, were caused by chemical groups from syndecan.

Fig. 2 shows the incorporation of extracts containing syndecan-4 in DPPC monolayers. This could be done by decompressing the monolayer from 30 mN/m to its maximum area and compressing it to collapse following the variation of surface pressure. This is important in order to better infer the behavior of syndecan in all possible surface densities, considering the heterogeneity of a surface membrane in terms of lateral pressure, fluidity, surface molecular packing, viscoelasticity and compressibility parameters. Also, it is reported that syndecans are encountered in several kinds of biointerfaces, including those that bear a great range of surface tensions, such as pulmonary alveolar cells [41,42]. For all extracts, a range of extract concentrations varying from 5 to 50 μg/L has been employed. In concentrations higher than 25 μg/L there were no more changes in the isotherms, representing that this concentration has a limit value. For this reason, for the sake of comparison, we show the curves reporting the effect of the extracts in the monolayer aqueous subphase always with the same concentration (25 μg/L). Clearly, we observe a more pronounced effect in the isotherms caused by EC and EJ-*ras* EC. The curves are shifted to larger DPPC molecular areas, proving the incorporation of some material from these extracts at the air–water interface. However, for shRNA-Syn4-EC, there is no significant change in the isotherms when compared to that for pure DPPC monolayer, where only an expansion of 1–3 $Å^2$/molecule at surface pressures around 10–15 mN/m, and a slight condensation of the monolayer at higher surface pressures were being observed. If we consider the surface pressure correspondent to that for a cell membrane [43], i.e. 30 mN/m, the isotherm shifted from 50 to 60 $Å^2$/molecule of DPPC for EC. This area corresponds not only to the area of the fraction of glycoprotein incorporated into the monolayer, but also is the effect from the lateral repulsion between the lipid alkyl chains and proteoglycan moieties. For the EJ-*ras* EC extract, the shift to larger areas is even higher, going from 50 to 65 $Å^2$/molecule of DPPC. It is believed that EJ-*ras* EC overexpresses syndecan-4 [37], while shRNA-Syn4-EC is silent, expressing no significant amounts of syndecan-4 [unpublished data]. These facts are a first indication that the expansion observed in the isotherms is owing to the heparan sulfate proteoglycan incorporated in the DPPC monolayer. Also, the surface elasticity changed considerably. The parameter that measures elasticity in Langmuir monolayers is known as surface compressional modulus, or in-plane elasticity, defined as $-1/A\ (d\pi/dA)_T$; [44], being A, the molecular area, and T the absolute temperature. This parameter drops from 280 mN/m for pure DPPC to 145 mN/m for DPPC–EJ-*ras* EC at a molecular area of 58 $Å^2$ as shown in Fig. 1B. The decrease is related to the effect of the fluidization of the monolayer caused by the molecules from the extract. For shRNA-Syn4-EC, however, we observe a more significant decrease of the surface elasticity, which

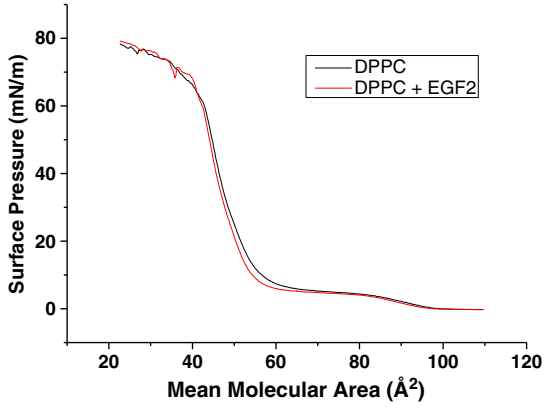

Fig. 3. Surface pressure-area isotherms for DPPC monolayer with EGF as aqueous subphase (25 μg/L).

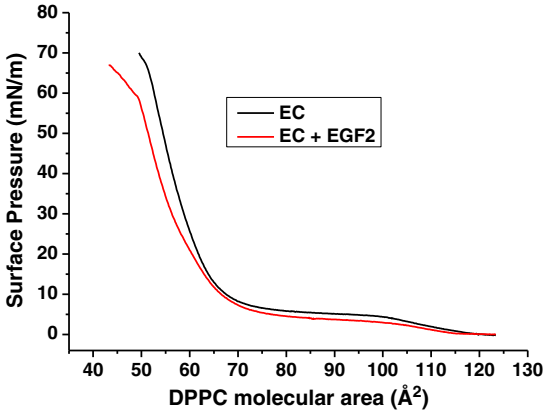

Fig. 4. Surface pressure-area isotherms for DPPC monolayers with EGF as subphase (25 μg/L) with or without EC (25 μg/L), as indicated in the inset.

goes to 78 mN/m, being in the range of the so-called liquid-ordered phases [44]. It is therefore reasonable to assume that the greater the amount of syndecan-4 adsorbed in the lipid monolayer, the more pronounced the effect in the packing properties of the Langmuir film.

Compression–decompression curves for the hybrid monolayer (see as example the curve in the inset of Fig. 2A) revealed that there are very slight displacements of the isotherms to lower molecular areas with successive cycles. Consequently, there is no hysteresis when comparing curves of compression and decompression, proving the thermodynamic stability of the monolayer.

As epidermal growth factors (EGF) are heparin-binding proteins that interact with cell surface associated with heparan sulfate proteoglycans, we have inserted EGF in the aqueous subphases of the monolayers produced in this work to investigate the process of molecular recognizing involving syndecan-EGF by means of tensiometry and infrared spectroscopy of hybrid syndecan–DPPC monolayers.

Firstly, we introduce EGF as subphase of pure DPPC monolayers to analyze the surface activity of this protein. In Fig. 3, we observe that EGF does not change significantly the isotherm for DPPC. Also the PM-IRRAS spectra (not shown) presented a straight line in the region of amide and sulfate groups (1700–1100 cm^{-1}), proving that EGF has a negligible surface activity to DPPC monolayers.

Fig. 4 shows that the growth factor, despite not influencing the isotherm for pure DPPC, decreases the surface pressure for the phase transition from liquid-expanded to liquid-condensed for EC–DPPC monolayers and shifts the isotherms to lower areas. This indicates that EGF does not penetrate in the hybrid proteoglycan-lipid monolayer. It is likely that the EGF interacts with the heparan sulfate chains of syndecan-4, implying that the heparan sulfate effects on cell growth are likely to be mediated by growth factors [8,45–49]. These chains may be localized in the subsurface just below the lipid–protein monolayer as portrayed in Fig. 5. The EGF–heparan sulfate interaction may relax the lipid–syndecan interaction owing to the polypeptide moiety buried into the DPPC monolayer. This molecular relaxation must cause the condensation of the monolayer, originating the shift to lower areas observed in the surface pressure-area isotherm. This relaxation is followed by an increase in the monolayer compressibility, which means that $d\pi/dA$ becomes higher for the monolayer with EGF when compared to the monolayer without EGF at surface pressures higher than 10 mN/m.

The PM-IRRAS spectra shown in Fig. 6 show slightly changes in the band positions for amide I, showing that the polypeptide moiety is little affected with EGF binding. Only a shift in the unordered band that goes from 1647 to 1644 cm^{-1}, as a probable indication of the relaxation between DPPC and the syndecan-4 moiety (transmembrane domain) buried in the lipid monolayer, as suggested in the model above. However, the region for sulfate and sugar changed drastically when compared to the spectra of Fig. 2. The bands for sulfate in

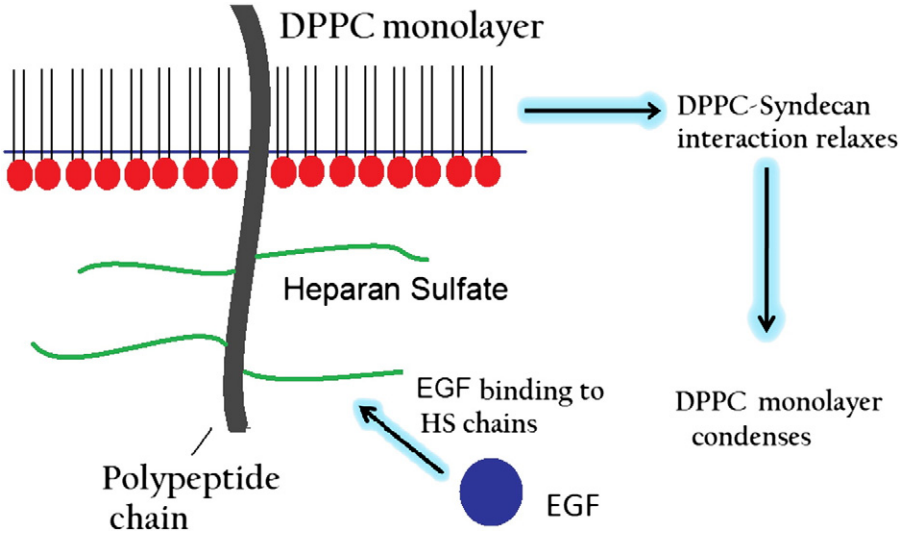

Fig. 5. Model for interaction of EGF with syndecan-4 in Langmuir monolayer. EGF binds to sulfate group in the heparan chain, which causes distortion in the polypeptide chain. The fraction of the polypeptide chain buried into the lipid monolayer relaxes the interface, condensing the lipid monolayer.

1263 and 1245 cm^{-1} were changed by a negative band at 1264 cm^{-1} at low surface pressures. With compression, this band goes to 1220 cm^{-1}, becoming positive. With compression, the relative intensity ($-I_1/I_2$) between the bands in 1264 cm^{-1} (I_1) and in 1220 cm^{-1} (I_2) decreases from 2.5 to 0.7, indicating that the EGF–sulfate interaction depends on the monolayer surface density. These results thus corroborate the fact that EGF interacts mainly with the sulfate group of the heparin sulfate chains of syndecan-4.

Figs. 7 and 8 confirm the hypothesis that EGF does not penetrate into the lipid monolayer, but should interact with the lateral chains of syndecan-4. This conclusion is gotten since there is an evident shift to lower molecular areas with EFG introduction, which reflects the over-expression of the proteoglycan in the EJ-*ras* EC extract. Also, the in-plane elasticity changed considerably, as shown in the inset for Fig. 7. The PM-IRRAS spectra show that the amide region is little affected. Now the unordered structure is better defined in 1650 cm^{-1} as the only consequence of EGF interaction, maybe reflecting the DPPC–polypeptide interaction relaxation caused indirectly by EFG binding in the extracellular domain. Again, the sulfate region is strongly affected showing the strong negative band at 1267 cm^{-1}. Additionally, a band at 1143 cm^{-1} is observed, which is attributed to sugar vibration transitions from the heparin sulfate chain.

It is important to call attention to the fact that the same experiments were essayed for shRNA-Syn4-EC and EGF, but no significant change was observed in the surface pressure-area isotherms and in the infrared spectra (not shown) other than those for shRNA-Syn4-EC/DPPC, corroborating the fact that the small amounts of the syndecan-4 in this extract will not affect the surface properties of the monolayer. Also, these results indicate that indeed the main molecule that causes surface activity in the monolayer is syndecam-4.

Finally, we have employed, instead of syndecan-4, heparin, a highly-sulfated glycoaminoglycan, whose chemical structure is quite similar to that for the heparam-sulfate chain linked to syndecam-4 (Figs. 9 and 10). Since it does not present hydrophobic domains as proteoglycans, the expansion of DPPC monolayer is less significant when compared to syndecans (EC and EJ-*ras* EC). However, as the EGF insertion in the aqueous suphase shifted the isotherms to lower molecular areas, it is likely that the interaction of heparin with EGF causes the removal of heparin from interface solubilizing the complex EGF-heparin to the subphase. Also, it is important to emphasize that heparin was not employed in this study to investigate syndecan–heparin interactions, but to comprehend, at the molecular level, the chemical groups involved in growth factor/sulfate glycoaminoglycan interactions by taking advantage of the chemical similarity between syndecan and heparin.

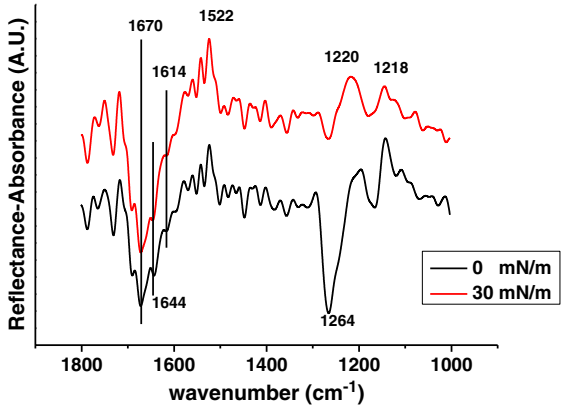

Fig. 6. PM-IRRAS spectra for DPPC monolayers at 30 mN/m on mixed EGF–EC (both at 25 μg/L) as subphase. Offset for clarity.

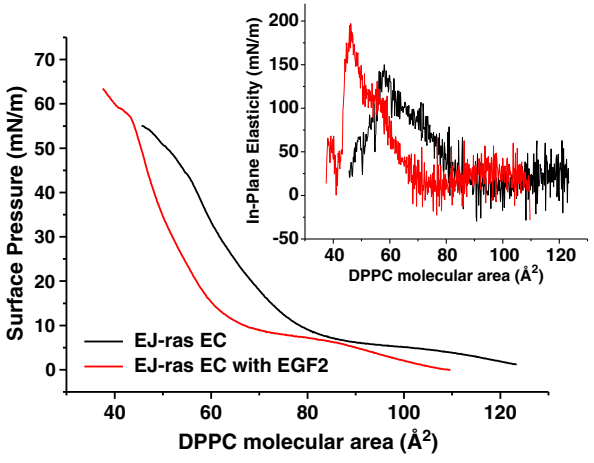

Fig. 7. Surface pressure-area isotherms for DPPC monolayers with growth factor as subphase without or with EJ-ras EC (25 μg/L) as indicated in the inset. Inset shows the In-Plane Elasticity-Area isotherms.

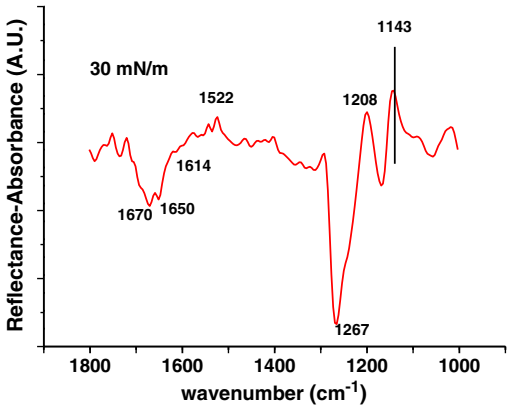

Fig. 8. PM-IRRAS spectra for DPPC monolayers at 30 mN/m with EJ-ras EC and growth factor as subphase.

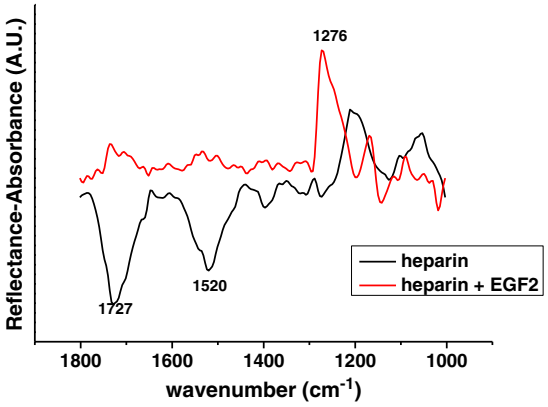

Fig. 10. PM-IRRAS spectra for DPPC monolayers at 30 mN/m with EGF (25 μg/mL) and heparin (25 μg/mL) as subphase. Offset for clarity.

PM-IRRAS spectra for heparin-DPPC show the band for S═O stretch at 1276 cm^{-1}, but no band for amide was observed. That is expected because polypeptide groups are absent. However a strong negative band is observed in 1727 cm^{-1}, related to C═O in DPPC, that can be attributed to the interaction of this group with heparin, which is reasonable because the polar affinity between these groups. The band in 1520 cm^{-1} is owing to the bending of H–O–H in water molecules that were replaced by heparin molecules in the subsurface for the DPPC monolayer. The spectra, taken when EFG was introduced, changes completely, as a proof for the remarkable interaction with heparin.

4. Conclusions

This paper shows that syndecan-4 is able to be incorporated in simplified model for the cell membrane outer layer at the air–water interface. Tumorigenic cells that express syndecan-4 expand the monolayer to higher lipid areas while silent cells for syndecan-4 do not. Growth factor presents no significant effect on the lipid monolayer without syndecan-4, but with the proteoglycan inserted in the lipid monolayer, it interacts somehow causing film condensation. This effect was explained by a model in which the growth factor links to the sulfate groups present in the glycan moiety of syndecan-4, which induces to chain of events that affects the polypeptide moiety buried in the lipid monolayer, causing its relaxation and resultant condensation. In conclusion, we believe that these results may have an important impact on the comprehension about the interaction of heparan sulfate proteoglycan involved in biochemical process at the level of cell membrane surfaces.

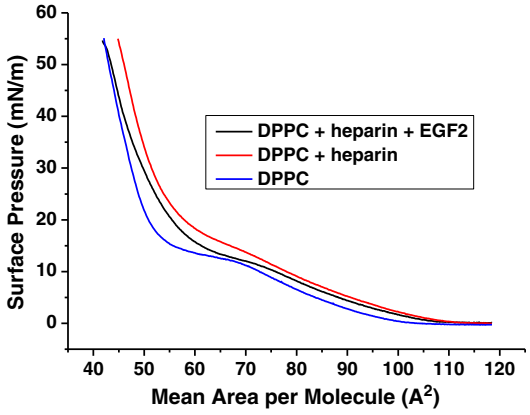

Fig. 9. Surface pressure-area isotherms for DPPC monolayers with EGF (25 μg/L) and heparin (25 μg/L) as subphase.

Acknowledgements

The authors acknowledge the support of FAPESP, CNPq, and CAPES-Nanobio: Filmes finos.

References

[1] C.P. Dietrich, H.B. Nader, A.H. Straus, Structural differences of heparan sulfates according to the tissue and species of origin, Biochem. Biophys. Res. Commun. 111 (1983) 865–871.
[2] C.P. Dietrich, I.L. Tersariol, L. Toma, C.T. Moraes, M.A. Porcionatto, F.W. Oliveira, H.B. Nader, Structure of heparan sulfate: identification of variable and constant oligosaccharide domains in eight heparan sulfates of different origins, Cell. Mol. Biol. (Noisy-le-grand) 44 (1998) 417–429.
[3] J.R. Couchman, L. Chen, A. Woods, Syndecans and cell adhesion, Int. Rev. Cytol. 207 (2001) 113–150.
[4] R. Chakravarti, J.C. Adams, Comparative genomics of the syndecans defines an ancestral genomic context associated with matrilins in vertebrates, BMC Genomics 7 (2006) 83.
[5] C.W. Kim, O.A. Goldberger, R.L. Gallo, M. Bernfield, Members of the syndecan family of heparan sulfate proteoglycans are expressed in distinct cell-, tissue-, and development-specific patterns, Mol. Biol. Cell 5 (1994) 797–805.
[6] M. Bernfield, M. Gotte, P.W. Park, O. Reizes, M.L. Fitzgerald, J. Lincecum, M. Zako, Functions of cell surface heparan sulfate proteoglycans, Annu. Rev. Biochem. 68 (1999) 729–777.
[7] M. Ueno, S. Yamada, M. Zako, M. Bernfield, K. Sugahara, Structural characterization of heparan sulfate and chondroitin sulfate of syndecan-1 purified from normal murine mammary gland epithelial cells. Common phosphorylation of xylose and differential sulfation of galactose in the protein linkage region tetrasaccharide sequence, J. Biol. Chem. 276 (2001) 29134–29140.
[8] C.C. Lopes, C.P. Dietrich, H.B. Nader, Specific structural features of syndecans and heparan sulfate chains are needed for cell signaling, Braz. J. Med. Biol. Res. 39 (2006) 157–167.
[9] H.A. Multhaupt, A. Yoneda, J.R. Whiteford, E.S. Oh, W. Lee, J.R. Couchman, Syndecan signaling: when, where and why? J. Physiol. Pharmacol. 60 (Suppl 4) (2009) 31–38.
[10] S. Choi, E. Lee, S. Kwon, H. Park, J.Y. Yi, S. Kim, I.O. Han, Y. Yun, E.S. Oh, Transmembrane domain-induced oligomerization is crucial for the functions of syndecan-2 and syndecan-4, J. Biol. Chem. 280 (2005) 42573–42579.
[11] I.C. Dews, K.R. Mackenzie, Transmembrane domains of the syndecan family of growth factor coreceptors display a hierarchy of homotypic and heterotypic interactions, Proc. Natl. Acad. Sci. U. S. A. 104 (2007) 20782–20787.
[12] E. Okina, T. Manon-Jensen, J.R. Whiteford, J.R. Couchman, Syndecan proteoglycan contributions to cytoskeletal organization and contractility, Scand. J. Med. Sci. Sports 19 (2009) 479–489.
[13] A. Woods, J.R. Couchman, Syndecan-4 and focal adhesion function, Curr. Opin. Cell Biol. 13 (2001) 578–583.
[14] A.C. Rapraeger, V.L. Ott, Molecular interactions of the syndecan core proteins, Curr. Opin. Cell Biol. 10 (1998) 620–628.
[15] J. Shin, W. Lee, D. Lee, B.K. Koo, I. Han, Y. Lim, A. Woods, J.R. Couchman, E.S. Oh, Solution structure of the dimeric cytoplasmic domain of syndecan-4, Biochemistry 40 (2001) 8471–8478.
[16] I. Langmuir, The constitution and fundamental properties of solids and liquids, J. Am. Chem. Soc. 39 (1917) 1848–1906.
[17] H. Brockman, Lipid monolayers: why use half a membrane to characterize protein–membrane interactions? Curr. Opin. Struct. Biol. 9 (1999) 438–443.
[18] A. Baszkin, Molecular recognition on the supported and on the air/water interface-spread protein monolayers, Adv. Colloid Interface Sci. 128–130 (2006) 111–120.

[19] A. Ariga, T. Nakanishi, J. Hill, A paradigm shift in the field of molecular recognition at the air–water interface: from static to dynamic, Soft Matter 2 (2006) 465–477.
[20] D. Vollhardt, Interfacial molecular recognition of non-surface-active species at Langmuir monolayers, Curr. Opin. Colloid Interface Sci. 13 (2008) 31–39.
[21] R.M. Leblanc, Molecular recognition at Langmuir monolayers, Curr. Opin. Chem. Biol. 10 (2006) 529–536.
[22] A.P. Girard-Egrot, S. Godoy, L.J. Blum, Enzyme association with lipidic Langmuir–Blodgett films: interests and applications in nanobioscience, Adv. Colloid Interface Sci. 116 (2005) 205–225.
[23] J.R. Siqueira, Jr., L. Caseli, F.N. Crespilho, V. Zucolotto, O.N. Oliveira, Jr., Immobilization of biomolecules on nanostructured films for biosensing, Biosens. Bioelectron. 25 1254–1263.
[24] R.M. Iost, J.M. Madurro, A.G. Brito-Madurro, I.L. Nantes, L. Caseli, F.N. Crespilho, Strategies of Nano-Manipulation for Application in Electrochemical Biosensors, Int J. Electrochem. Sci. 6 (2011) 2965–2997.
[25] P. Alessio, F.J. Pavinatto, O.N. Oliveira, Jr., J.A. De Saja Saez, C.J. Constantino, M.L. Rodriguez-Mendez, Detection of catechol using mixed Langmuir–Blodgett films of a phospholipid and phthalocyanines as voltammetric sensors, Analyst 135 2591–2599.
[26] R. Maget-Dana, The monolayer technique: a potent tool for studying the interfacial properties of antimicrobial and membrane-lytic peptides and their interactions with lipid membranes, Biochim. Biophys. Acta 1462 (1999) 109–140.
[27] M.C. Colhone, M.E.D. Zaniquelli, P. Ciancaglini, R.G. Stabeli, J.R.S.A. Leite, V. Zucolotto, Dermaseptin 01 as antimicrobial peptide with rich biotechnological potential: study of peptide interaction with membranes containing *Leishmania amazonensis* lipid-rich extract and membrane models, J. Pept. Sci. 17 (2011) 700–707.
[28] A.B. Lopez-Oyama, P. Taboada, M.G. Burboa, E. Rodriguez, V. Mosquera, M.A. Valdez, Interaction of the cationic peptide bactenecin with mixed phospholipid monolayers at the air–water interface, J. Colloid Interface Sci. 359 (2011) 279–288.
[29] J. Strzalka, J. Liu, A. Tronin, I.Y. Churbanova, J.S. Johansson, J.K. Blasie, Mechanism of interaction between the general anesthetic halothane and a model ion channel protein, I: Structural investigations via X-Ray reflectivity from Langmuir monolayers, Biophys. J. 96 (2009) 4164–4175.
[30] Y. Negishi, D. Omata, H. Iijima, N. Hamano, Y. Endo-Takahashi, M. Nomizu, Y. Aramaki, Preparation and characterization of laminin-derived peptide AG73-coated liposomes as geny delivery tool, Biol. Pharm. Bull. 33 (2010) 1766–1769.
[31] A. Wang, T. Miralem, D.M. Templeton, Heparan sulfate chains with antimitogenic properties arise from mesangial cell-surface proteoglycans, Metabolism 48 (1999) 1220–1229.
[32] Y.L. Lopez-Franco, M.A. Valdez, J. Hernandez, A.M. Calderon de la Barca, M. Rinaudo, F.M. Goycoolea, Macromolecular dimensions and mechanical properties of monolayer films of Sonorean mesquite gum, Macromol. Biosci. 4 (2004) 865–874.
[33] H.V. Patel, A.A. Vyas, K.A. Vyas, Y.S. Liu, C.M. Chiang, L.M. Chi, W. Wu, Heparin and heparan sulfate bind to snake cardiotoxin. Sulfated oligosaccharides as a potential target for cardiotoxin action, J. Biol. Chem. 272 (1997) 1484–1492.
[34] H.A. Santos, V. Garcia-Morales, R.J. Roozeman, J.A. Manzanares, K. Kontturi, Interfacial interaction between dextran sulfate and lipid monolayers: an electrochemical study, Langmuir 21 (2005) 5475–5484.
[35] T.M. Nobre, F.J. Pavinatto, M.R. Cominetti, H.S. Selistre de-Araujo, M.E. Zaniquelli, L.M. Beltramini, The specificity of frutalin lectin using biomembrane models, Biochim. Biophys. Acta (1798) 1547–1555.
[36] V. Buonassisi, J.C. Venter, Hormone and neurotransmitter receptors in an established vascular endothelial cell line, Proc. Natl. Acad. Sci. U. S. A. 73 (1976) 1612–1616.
[37] C.C. Lopes, L. Toma, M.A.S. Pinhal, M.A.S. Porcionatto, M.C. Sogayar, C.P. Dietrich, H.B. Nader, EJ-ras oncogene transfection of endothelial cells upregulates the expression of syndecan-4 and downregulates heparan sulfate sulfotransferases and epimerase, Biochimie 88 (2006) 1493–1504.
[38] H.B. Nader, V. Buonassisi, P. Colburn, C.P. Dietrich, Heparin stimulates the synthesis and modifies the sulfation pattern of heparan sulfate proteoglycan from endothelial cells, J. Cell. Physiol. 140 (1989) 305–310.
[39] W.P. Ulrich, H. Vogel, Polarization-modulated FTIR spectroscopy of lipid/gramicidin monolayers at the air/water interface, Biophys. J. 76 (1999) 1639–1647.
[40] Y. Halden, A. Rek, W. Atzenhofer, L. Szilak, A. Wabnig, A.J. Kungl, Interleukin-8 binds to syndecan-2 on human endothelial cells, Biochem. J. 377 (2004) 533–538.
[41] J. Pruessmeyer, C. Martin, F.M. Hess, N. Schwarz, S. Schmidt, T. Kogel, N. Hoettecke, B. Schmidt, A. Sechi, S. Uhlig, A. Ludwig, A disintegrin and metalloproteinase 17 (ADAM17) mediates inflammation-induced shedding of syndecan-1 and -4 by lung epithelial cells, J. Biol. Chem. 285 (2010) 555–564.
[42] C.R. Kliment, J.M. Englert, B.R. Gochuico, G. Yu, N. Kaminski, I. Rosas, T.D. Oury, Oxidative stress alters syndecan-1 distribution in lungs with pulmonary fibrosis, J. Biol. Chem. 284 (2009) 3537–3545.
[43] D. Marsh, Lateral pressure in membranes, Biochim. Biophys. Acta 1286 (1996) 183–223.
[44] J.T. Davies, E.K. Rideal, Interfacial Phenomena, 2nd ed. Academic Press, New York, 1963.
[45] J.J. Castellot Jr., D.L. Beeler, R.D. Rosenberg, M.J. Karnovsky, Structural determinants of the capacity of heparin to inhibit the proliferation of vascular smooth muscle cells, J. Cell. Physiol. 120 (1984) 315–320.
[46] J.A. Thompson, K.D. Anderson, J.M. DiPietro, J.A. Zwiebel, M. Zametta, W.F. Anderson, T. Maciag, Site-directed neovessel formation in vivo, Science 241 (1988) 1349–1352.
[47] A. Yayon, M. Klagsbrun, J.D. Esko, P. Leder, D.M. Ornitz, Cell surface, heparin-like molecules are required for binding of basic fibroblast growth factor to its high affinity receptor, Cell 64 (1991) 841–848.
[48] K. Matsuda, H. Maruyama, F. Guo, J. Kleeff, J. Itakura, Y. Matsumoto, A.D. Lander, M. Korc, Glypican-1 is overexpressed in human breast cancer and modulates the mitogenic effects of multiple heparin-binding growth factors in breast cancer cells, Cancer Res. 61 (2001) 5562–5569.
[49] Y. Song, D.C. McFarland, S.G. Velleman, Fibroblast growth factor 2 and protein kinase C alpha are involved in syndecan-4 cytoplasmic domain modulation of turkey myogenic satellite cell proliferation, Comp. Biochem. Physiol. A Mol. Integr. Physiol. 161 (2012) 44–52 [Electronic publication ahead of print].